

MIXED CONVECTION COOLING OF MULTIPLE PROTRUDING HEAT SOURCES IN A HORIZONTAL CHANNEL

انتقال الحرارة بالحمل المختلط من عدة منابع حرارية بارزة في مجرى أفقية

G. I. Sultau

Mechanical Power Engineering Department
El Mansoura University, Egypt

الخلاصة :

يتناول البحث دراسة معملية لانتقال الحرارة بالحمل المختلط للهواء من ثلاثة منابع حرارية مسطحة بارزة ذات فيض حراري ثابت ومثبتة على سطح أفقي معزول لمجرى هوائي مستطيل المقطع. وتظهر أنه مع زيادة الدراسة في تبريد الأجهزة الإلكترونية ومحولات الجهد العالي. وتركز هذه الدراسة على اعتماد خصائص انتقال الحرارة وأقصى درجة حرارة لسطح المنابع الحرارية على رقم رينولدز ، ورقم ريتشاردسون. أثناء التجارب تم تغيير رقم رينولدز في المدى من 135.9 إلى 7221.5 ومعامل الطفو رقم ريتشاردسون تغير من 0.0406 إلى 24.4 . كما تضمنت الدراسة تأثير نسبة المسافة بين المنابع الحرارية إلى عرض المنبع $s/\text{spacing/heater}$ "length ratio" على خصائص انتقال الحرارة داخل مجرى الهواء وقد تغيرت هذه النسبة من 0.5 إلى 3.0 . وقد وجد أن نوسنت المتوسط يزيد بزيادة كل من نسبة المسافة بين المنابع الحرارية إلى عرض المنبع الواحد وكذلك وزيادة رقم رينولدز ، ودرجة الحرارة القصوى على سطح المسخنات تحددت عند الحافة السفلية للسطح الخلفي لكل مسخن . كما أظهرت الدراسة ، أنه ليس هناك حاجة لزيادة s/L عن الواحد عندما يكون رقم رينولدز أكبر من 1720 والذي يناظر في حالتنا هذه سرعة سريان أكبر من 1.0 m/s . وقد استنتجت علاقات رياضية تربط كل من درجة الحرارة القصوى لسطح المسخنات ومعامل انتقال الحرارة المتوسط مع رقم ريتشاردسون ونسبة المسافة بين المسخنات إلى عرض المسخن .

ABSTRACT:

Heat transfer characteristics due to mixed convection from three protruding heat sources mounted on a horizontal adiabatic surface of an air rectangular channel is investigated experimentally. The investigation is concentrated on the dependence of heat flow characteristics and maximum heater surface temperature on Reynolds number and Grashof number as well as Richardson number. During the experiments, the Reynolds number ranges from 135.9 to 7221.5 and the buoyancy parameter, Richardson number, Gr/Re^2 , ranges from 0.0406 to 24.5. The experiments are extended to study the effect of spacing between the heat sources for spacing-heater length ratio $s/L = 0.5, 1.0, 2.0$ and 3.0 , for $b/L=0.59$ on heat flow characteristics and maximum surface temperature. θ_{max} occurs at the lower edge points of the right face of each heater. With the increase of Reynolds number the effect of s/L ratio on θ_{max} decreases and there is no need to increase s/L over 1 for $Re > 1720$ which gives (in this case) flow velocity $> 1 \text{ m/s}$. Also, θ_{max} and \bar{Nu} are correlated with Gr/Re^2 and s/L ratio for the three heaters.

INTRODUCTION:

In recent years, heat transfer in microelectronics equipment has received considerable attention from the heat transfer researchers. Unless an effective removal of the excessive heat generated within the devices in place, the performance of these sensitive electronic devices deteriorates rapidly. The trend in the electronic industry has been directed towards smaller components "ICs" which are mounted in a dense-packed rows on the printed circuit (board), the spacing between each two rows and the position of the higher power dissipating component within the package should be optimised as to maximise the forced convection heat transfer within the enclosure.

Although a number of papers have been published in the general area of convective cooling of electronic components, a little work has been carried out for simulating protruding heat sources on an adiabatic horizontal surface. In both forced and natural convection heat transfer fields, the literature supplies some work dealing with the cooling of heat sources. Among them the works of Ramadhani et al., [1], Incropera et al. [2], Davalath and Bayazitoglu [3], Wadsworth and Mudawar [4], Kim and Anand [5], Molki et al. [6], Hwang and Liou [7], Nakayama and Park [8], Fowler et al. [9], EL-Kady and Araid [10], and EL-Kady [11].

Large number of practical situations involve mixed convective heat transfer in which both modes of forced and natural convection effects are dominant and both modes are significant. Such circumstances arise when a fluid flows over a heated surface with relatively low velocity. Habchi and Archarya [12], constructed a numerical investigation for mixed convection of air in a vertical channel containing partial rectangular blockage on one channel wall. The wall containing the blockage was assumed to be heated while the other wall was assumed to be adiabatic. Maughan and Incropera [13] made experimental measurements in the thermal entry for various channel inclinations. Mahaney et al. [14] studied the mixed convective heat transfer from an array of discrete heat sources in a horizontal rectangular channel. An analysis is made by Kim et al. [15] of the flow and heat transfer characteristics of a mixed convection from multiple-layered boards with cross-streamwise periodic boundary conditions. Papanicolaou and Jaluria [16], simulated numerically the combined forced and natural convective cooling of heat dissipating surface, located in the walls of a rectangular cavity, and cooled by an upper external through flow of air. EL-Kady and Sultan [17], developed a theoretical and experimental study for mixed convection heat transfer on a single protruding heat source mounted on a horizontal adiabatic surface of a rectangular channel.

The present experimental work investigated the heat transfer characteristics due to mixed convection from three protruding heat sources mounted on a horizontal adiabatic surface of a rectangular channel. The dependence of the heat flow characteristics and the maximum surface temperature on Reynolds number and Grashof number as well as the Richardson number are investigated. The analysis is extended to study the effect of spacing between heat sources for spacing/heater length ratio $s/L = 0.5, 1.0, 2.0$ and 3.0 on heat flow characteristics. Correlation for heat flow characteristics and maximum surface temperature with Richardson number and spacing ratio are obtained.

3.1.7.1. HORIZONTAL WORK:

The details of the experimental test section are shown in Fig.1, an a schematic diagram of experimental apparatus is shown in Fig.2. A low speed wind tunnel with $12 \times 12 \text{ cm}^2$ square section and 60 cm long (1) made from perspex is used. The air enters the test section through a bell mouth inlet (2) and a fine mesh screen (3) to ensure a fairly uniform flow with a negligible turbulence in the test section. The local flow velocity is measured by means of a hot wire anemometer (4) at different locations in both Y and Z directions in a section free of the blockage heaters and is integrated to get the average air velocity.

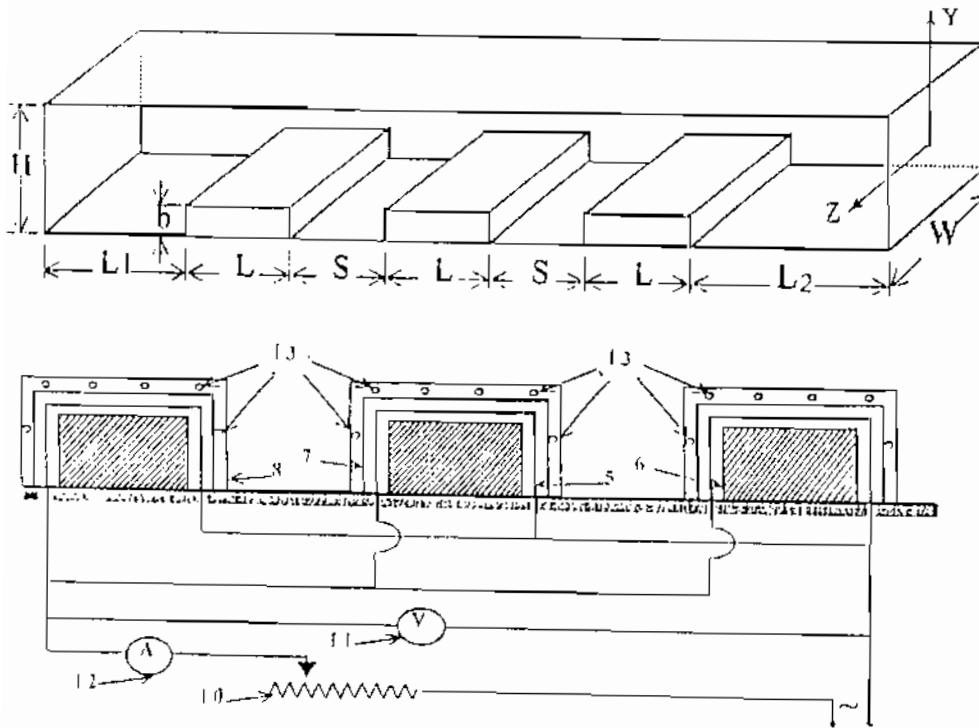


Fig.1 Details of test section

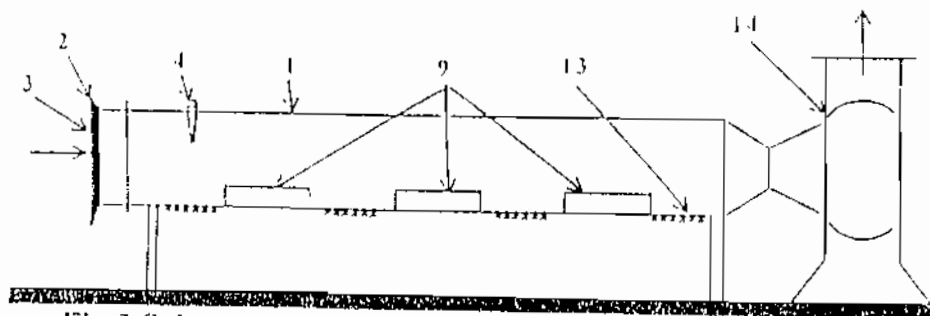


Fig.2 Schematic diagram of the experimental apparatus.

(1) Test section, (2) Bell mouth, (3) Fine mesh screen, (4) Hot wire anemometer, (5) Nickel chrommum electric heater, (6) granite case, (7) Mica sheet, (8) Aluminum channel, (9) Heat source module, (10) Variac transformer, (11) Voltmeter, (12) Ammeter, (13) copper constantan thermocouple, and (14) Blow-off.

Three typical heat sources (9) of 2.7 cm wide, 1.6 cm height and 12 cm long are mounted firmly on the floor of the test section at a spacing ratio S/L varied from 0.5 to 3.0 to form the three protruding blockage heaters. Each heat source is made of a nickel-chromium wire (5) which is wrapped at equal pitches over a ceramic core (6) of 2.2 cm wide, 1.4 cm height and 12 cm long, as shown in Fig.1. Each core is surrounded by mica-sheet of 0.5 mm thickness (7) and inserted inside a highly polished aluminium channel (8) of 2.72cm wide, 1.64 cm height and 12 cm long to form protruding heat sources.

The heat input to the heaters is controlled by using an autotransformer (10) as well as an ammeter (12) and voltmeter (11). The surface temperature of each heater is measured by means of 6 copper constantan thermocouples (13) which were made of 0.25 mm diameter and attached to the inside surface of the aluminium channels by means of a highly thermal conductivity cement. The temperature distribution along the floor surface is measured by another 24 copper-constantan thermocouples as shown in Fig.2. The thermocouples are connected to a digital temperature recorder with a sensitivity of 0.1°C . Nearly two hours were needed to reach the steady state condition which was recorded as temperature reading did not change within a time of about 10 minutes.

Results of heat source and the base adiabatic floor are presented in terms of the local and maximum temperature, as well as the local and average Nusselt numbers which are defined as:

$$\text{Nu} = h L/k = q L/(T - T_o) k \quad (1)$$

$$\bar{\text{Nu}} = \bar{q} L / (\bar{T} - T_o) k \quad (2)$$

Where Nu and $\bar{\text{Nu}}$ are the local and average Nusselt number

T and \bar{T} are the local and average surface temperature respectively

T_o free stream air temperature,

k is the fluid thermal conductivity,

L is the heater length

Reynolds number, Grashof number and Richardson number are defined as follows:

$$\text{Re} = u_o L/v,$$

$$\text{Gr} = g \beta q (L+2 b)L^3 / (k v^2),$$

$$\text{Ri} = \text{Gr}/\text{Re}^2$$

Where u_o is the average air flow velocity through the channel cross section

v is the kinematic viscosity of the air,

β is the volumetric coefficient of thermal expansion

The dimensionless local heater surface temperature θ is defined as:

$$\theta = [(T - T_o)/(q_o L/k)] \cdot \text{Gr}^{0.2} \quad (3)$$

RESULTS AND DISCUSSION:

The basic physical parameters of the problem under consideration are heat flux q , heater width L , heater height b , height of the test section H the distance L_1 from the leading edge, the distance L_2 from the third block to the exit of the test section, the distance s between each two blocks, and the velocity u_o . The relevant dimensionless

quantities may be derived from these physical variables as $L_1/L=10$, $L_2/L=10$, 11, 12 and 13, $t/L=4.4$, $b/L=0.59$, S/L varies from 0.5 to 3 with operating parameters of $Pr=0.7$, $Gr=0.403 \times 10^7$ and $135 < Re < 7221.5$.

The results presented here include dimensionless maximum and local temperature distribution profiles and average and local Nusselt number distribution. Also, the regions of natural convection dominated flow, transient flow and forced convection dominated flow are determined in terms of Reynolds number Re , and Richardson number $Ri=Gr/Re^2$.

Temperature Distribution:

The local temperature distribution across the test section is presented in Fig. (3) for Grashof number = 0.403×10^7 , fixed values of Reynolds number ranging from $Re=135-7221.5$ and spacing ratio $s/L=2.0$. The local surface temperature decreases with increasing Reynolds number for the three faces of each heater as well as the adiabatic floor surface. The local surface temperature of the first heater is lower than that of the second one and the local temperature of the second heater is lower than that of the third one for $Re \geq 1720$. At the right face of each heater, θ increases in the direction towards the bottom corner due to the flow separation and wake effects, making θ_{max} occurs at the bottom corner points D, H, and L. While θ at the left face of each heater decreases in the direction towards the top edge of each heater.

Figure 4 shows the influence of Reynolds number on the max. temperature of the three heaters which occur at points D, H, and L respectively. For low Reynolds number, mainly $Re=136-376$, the max. temperature occurs at the middle heater, this is because the flow is mainly natural convection dominated. For $Re=378$, θ_{max} at both the middle and third heater is nearly the same. With the increase of Reynolds number $700 \leq Re \leq 3000$, θ_{max} moves with the flow to the last heater. For $Re \geq 3000$, with the increase of Reynolds number, the maximum temperature of the three heaters tends to be nearly the same.

Heat Transfer:

The variation of the local Nusselt number along the heater's surfaces is shown in Fig. (5) for different values of Reynolds number, while, Fig. 6 presents the behaviour of the average Nusselt number with Reynolds number for the three heaters. The heat transfer from the heaters to the fluid increases as Reynolds number increases. The maximum heat transfer rate occurs near the front top edge of each block, followed by a gradual decay at the top surface until the point of maximum temperature, then followed by another gradual increase until the trailing edge of the top face. At the right faces, gradual decrease is observed from the top edge point to the bottom corner point, which has the minimum rate of heat transfer.

Effect of Spacing between the Heaters

The analysis is extended to study the effect of spacing between the heaters, for spacing/heater length ratios $s/L=0.5, 1.0, 2.0$ and 3.0 . The variation of the surface

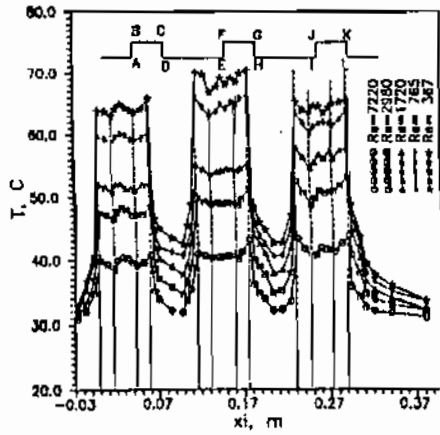


Fig.3 The variation of local surface temperature with x_i at different Reynolds number for $s/L=2.0$, $b/L=0.59$, $H/L=4.4$, $L_1=L_2=10$, $Pr=0.7$ and $Gr=0.403E+7$, $T_0=28^\circ C$

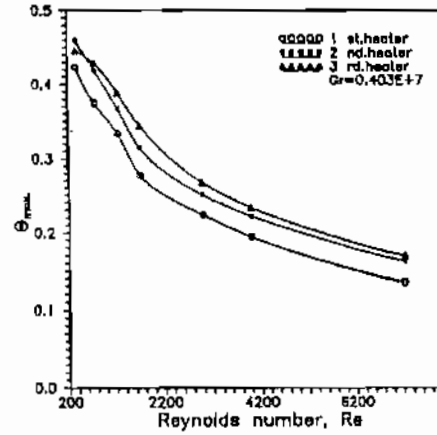


Fig.4 Variation of maximum heaters surface temperature with Reynolds number for $s/L=2$, $b/L=0.59$, $H/L=4.4$, $L_1/L=L_2/L=10$ and $Pr=0.7$

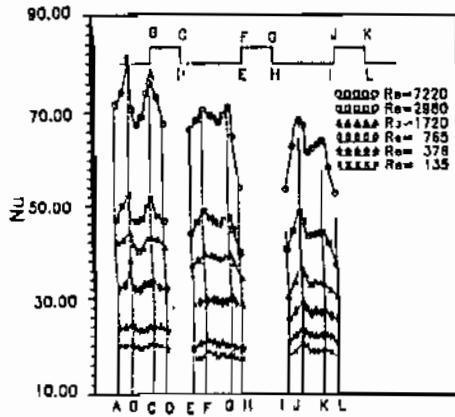


Fig.5 Influence of heater's locations on the local Nusselt number for $s/L=2.0$, $b/L=0.59$, $H/L=4.4$, $L_1=L_2=10$, $Pr=0.7$ and $Gr=0.403E+7$.

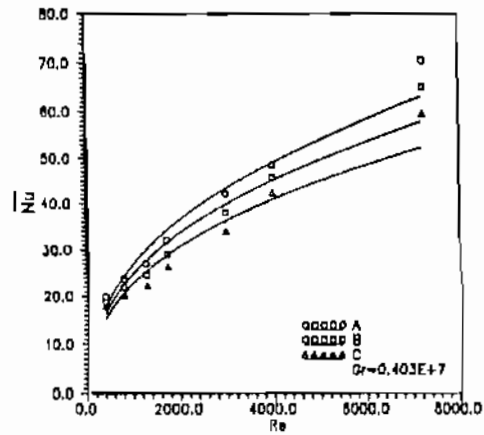


Fig.6 The mean Nusselt number of the three heaters versus Reynolds number for $s/L=2.0$, $b/L=0.59$, $H/L=4.4$, $L_1/L=10$, $L_2/L=12$ and $Pr=0.7$.

temperature and local Nusselt number along the surfaces of the three heaters is shown in Figs 7 and 8. The local temperature distribution and local Nusselt number of the first heater did not change with s/L along the surface until $s/L=1.417$ (near the backward edge) at which the local surface temp. begin to increase with decreasing spacing/heater length ratio, while the local nusselt number begins to decrease with decreasing spacing/heater length ratio. But for the second and third heaters, the local temperature increases with decreasing the spacing/heater length ratio while the local Nusselt number decreases with decreasing that ratio. The location of the points of maximum temperatures and points of maximum local Nusselt number did not change along the three surfaces of each heater with the variation of the spacing ratio.

Figure 9 shows the variation of dimensionless max. surface temperature θ_{max} of the three heaters with Reynolds number, Re , at various spacing ratios. θ_{max} decreases with increasing Reynolds number and with increasing the spacing ratio. With the increase of Reynolds number the curves of θ_{max} for different values of s/L converge indicating that with further increase of Reynolds number, the effect of s/L ratio on Nu decreases.

Figures 10 show the variation of dimensionless maximum surface temperature θ_{max} of the three heaters with Richardson number Gr/Re^2 at various spacing ratios. θ_{max} increases with increasing Richardson number.

Figure 11 shows the behaviour of average Nusselt number \bar{Nu} with spacing ratio s/L for the three heaters at fixed values of Reynolds number; $Re = 135, 1720, 2790,$ and 3980 . For Low Reynolds number, $Re = 135$, \bar{Nu} increases with increased rate with the increase of the spacing ratio s/L . This is because, this case corresponds to airflow velocity $u_a = 0.075$ m/s, which is natural dominated flow, so with the increase of the spacing between the heaters, the temperatures decrease and the Nusselt number increases. The Figure shows also that with the increase of Reynolds number the effect of forced convection part increases, therefore, the effect of increasing the spacing ratio on the variation of Nusselt number decreases. For $Re=1720$ which corresponds to $u_a=1$ m/s, the change of s/L from 1 to 3 causes an increase of Nu by about 3%. For $Re=3980$ which is corresponding to $u_a = 2.3$ m/s, the increase of s/L from 0.5 to 3 causes an increase of Nu by about 2% and the increase of s/L from 1 to 3 causes an increase of Nu by about 1%. This result gives that, there is no need to increase s/L over 1 for Reynolds number ≥ 1720 which gives flow velocity ≥ 1 m/s.

The dependence of mean Nusselt number for the three heaters on Reynolds number is shown in Fig 12 for different values of s/L . \bar{Nu} increases with increasing both Reynolds number and s/L ratio. Figure 13 indicate the dependence of average Nusselt number of the three heaters with Richardson number Gr/Re^2 for different s/L ratios. In the natural convection dominated flow $Gr/Re^2 > 8.0$, \bar{Nu} decreases slightly with increasing Richardson number while in the forced convection dominated flow $Gr/Re^2 < 0.1$ the mean Nusselt number decreases dramatically with increasing of Gr/Re^2 . In the transition region, mean Nusselt number decreases sharply with increasing Gr/Re^2 for the different values of aspect ratio.

An attempt was made to correlate the present experimental data to obtain the dependence of the maximum surface temperature θ_{max} with Gr/Re^2 and mean Nusselt number on Richardson number $[Gr/Re^2]$ and aspect ratio s/L . Drawing the curves of

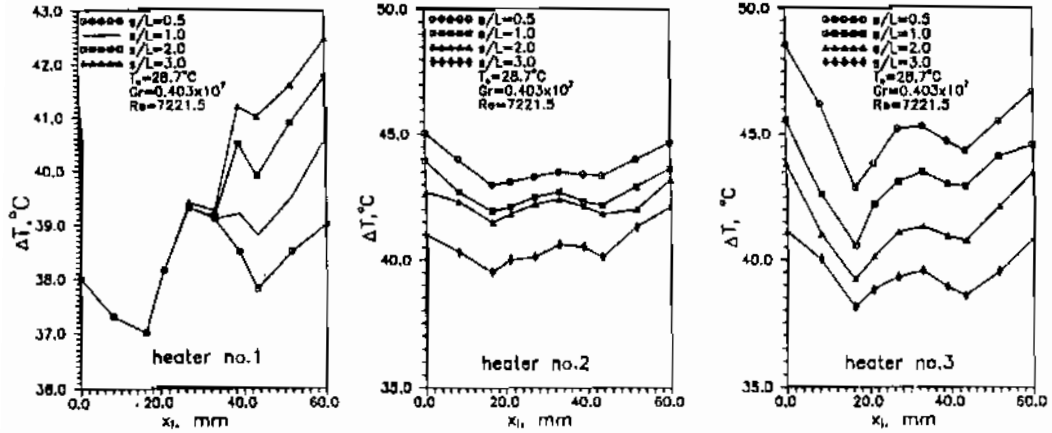


Fig.7 Variation of local surface temperature with position along the surface of the three heaters at different spacing/length ratio and constant both Re and Gr.

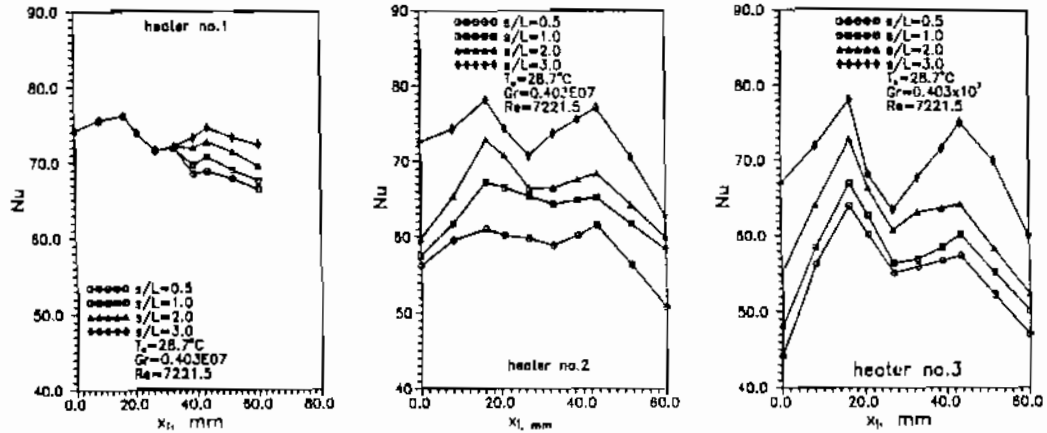


Fig.8 Variation of local Nusselt number with position along the surface of the heaters at different spacing/heater length ratio and constant both Re and Gr.

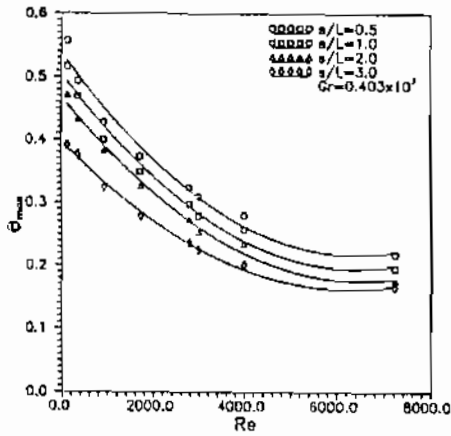


Fig.9 Variation of max. temperature distribution of the three heaters with Re at different spacing/heater length ratio and constant Gr.

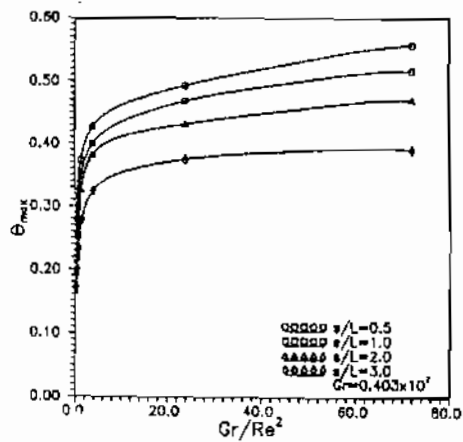


Fig.10 Variation of max. temperature distribution of the heaters with Gr/Re^2 at different spacing/heater length ratio and constant Gr.

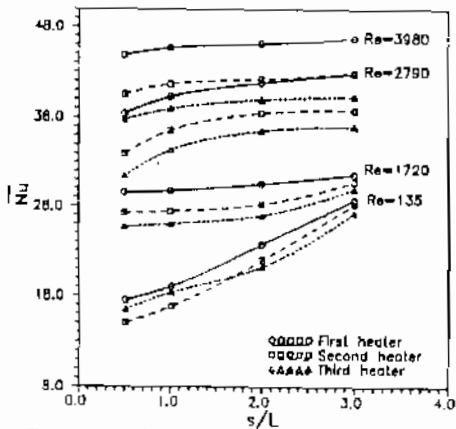


Fig.11 Variation of mean Nusselt number with spacing/heater length ratio at constant Gr.

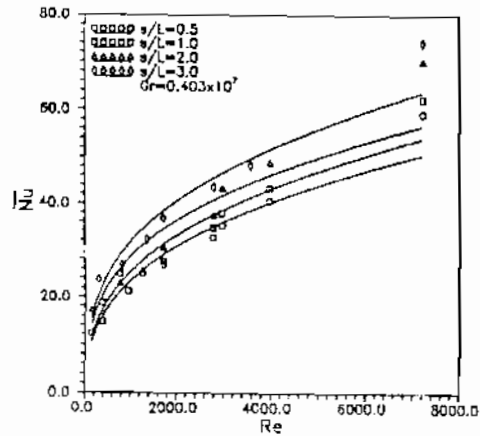


Fig.12 Variation of mean Nusselt number of the three heaters with Re at different spacing/heater length ratio and constant Gr.

both $[\theta_{\max} / (Gr/Re^2)^a]$, $Nu/(Gr/Re^2)^b$ against s/L , a correlation for maximum temperature and mean Nusselt number can be found from Figs.14 and 15 as follows:

$$\theta_{\max} = [0.383-0.093(s/L)+0.016(s/L)^2] \cdot (Gr/Re^2)^{0.128} \quad (4)$$

$$\bar{Nu}_1 = [35.653-2.55(s/L)+1.54(s/L)^2](Gr/Re^2)^{-0.2235} \quad (5)$$

$$\bar{Nu}_2 = [31.81-1.77(s/L)+1.59(s/L)^2](Gr/Re^2)^{-0.2165} \quad (6)$$

$$\bar{Nu}_3 = [31.01-3.18(s/L)+1.59(s/L)^2](Gr/Re^2)^{-0.2001} \quad (7)$$

for $b/L=0.59$, $135.9 < Re < 7221.5$, $0.0406 < Gr/Re^2 < 24.5$

CONCLUSIONS :

Heat transfer characteristics due to mixed convection from three protruding heat sources mounted on a horizontal adiabatic surface of a rectangular channel is investigated experimentally. The investigation concentrated on the dependence of the heat flow characteristics and the maximum surface temperature on Reynolds number and Grashof number as well as the Richardson number. The analysis is extended to study the effect of spacing between the heat sources for spacing/heater length ratio $s/L = 0.5, 1.0, 2.0$ and 3.0 for $b/L=0.59$, $135.9 < Re < 7221.5$, $0.0406 < Gr/Re^2 < 24.5$, and the following conclusions are obtained:

The local surface temperature decreases with increasing Reynolds number for the three faces of each heater as well as the adiabatic floor surface. At the right face of each heater, θ_{\max} occurs at the lower corner points, while θ at the left face of each heater decreases in the direction towards the top edge of each heater.

For natural convection dominated flow, θ_{\max} occurs at the middle heater. For transient dominated flow region, θ_{\max} occurs at both the middle and third heater, while for $700 \leq Re \leq 3000$, θ_{\max} moves with the flow to the third (last) heater.

The heat transfer from the heaters to the fluid increases as Reynolds number increases. The maximum heat transfer occurs near the front top edge of each block. At the right faces, gradual decrease is observed from the top edge point to the bottom corner point, which has the minimum rate of heat transfer.

With the increase of s/L the local temperature decreases, the local Nusselt number increases and θ_{\max} decreases. With the increase of Reynolds number the values of θ_{\max} for different values of s/L converge indicating that with further increasing of Reynolds number, the effect of s/L ratio on Nu decreases.

For natural dominated flow, \bar{Nu} increases with the increase of the spacing ratio s/L . With the increase of Reynolds number, the effect of increasing the spacing ratio on the variation of \bar{Nu} decreases, and there is no need to increase s/L over 1 for $Re \geq 1720$ which gives flow velocity $\geq 1 \text{ m/s}$.

θ_{\max} and \bar{Nu} are correlated with Gr/Re^2 and s/L for the three heaters as follows:

$$\theta_{\max} = [0.383-0.093(s/L)+0.016(s/L)^2] \cdot (Gr/Re^2)^{0.128}$$

$$\bar{Nu}_1 = [35.653-2.55(s/L)+1.54(s/L)^2](Gr/Re^2)^{-0.2235}$$

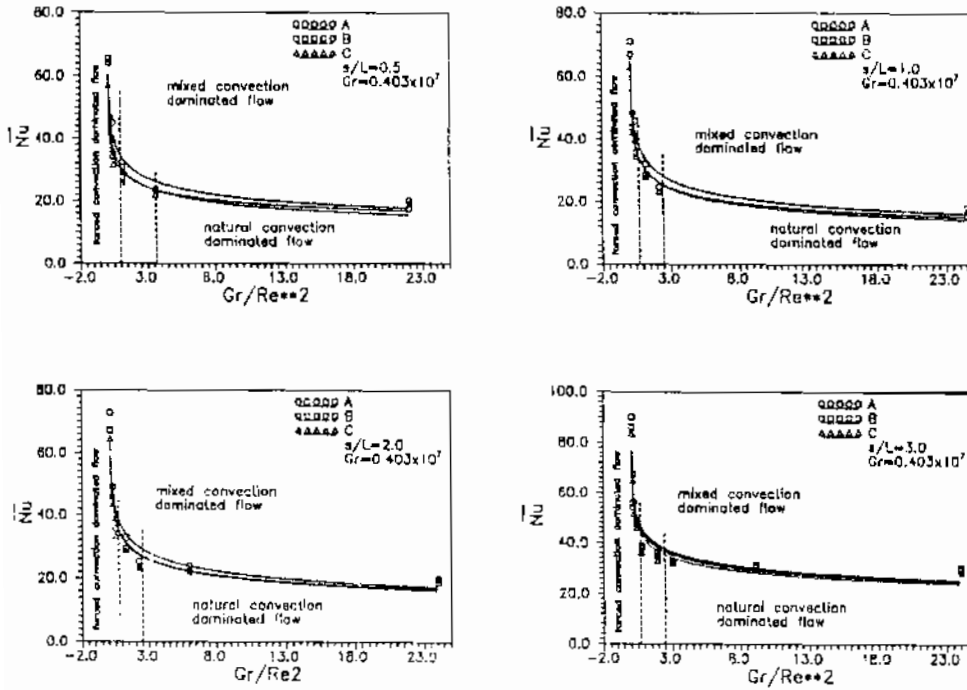


Fig.13 Variation of average Nusselt number with Gr/Re^2 for different spacing/heater length ratio $s/L=0.59$, $H/L=4.44$ and $L_1/L=10$.

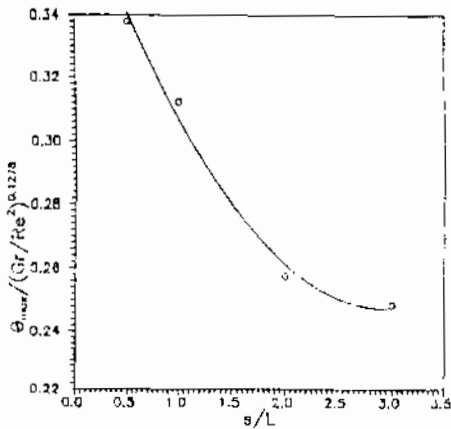


Fig.14 Correlation of max. dimensionless temp. distribution of the heaters with spacing/heater length ratio.

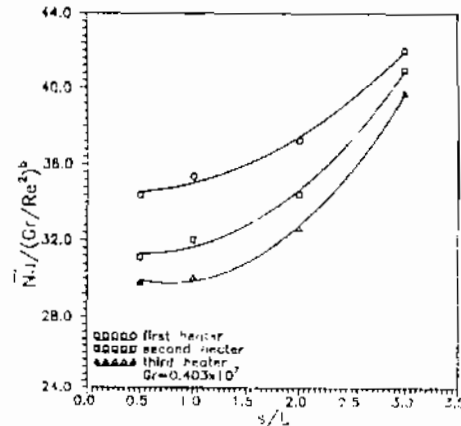


Fig.15 Correlation of the present experimental data with spacing/heater length ratio at constant Grashof number

$$\bar{Nu}_2 = [31.81 - 1.77(s/L) + 1.59(s/L)^2](Gr/Re^2)^{0.2165}$$

$$\bar{Nu}_3 = [31.01 - 3.18(s/L) + 1.59(s/L)^2](Gr/Re^2)^{0.2}$$

for $b/L=0.59$, $135.9 < Re < 7221.5$, $0.0406 < Gr/Re^2 < 24.5$

NOMENCLATURE :

A, B, C, D	corner points of the first heater
E, F, G, H	corner points of the second heater
I, J, K, L	corner points of the third heater
b	heater height, m
b_1	exponent of eqs.
h	convective heat transfer coefficient, $W/m^2.K$
Gr	Grashof number, $Gr = g \beta q (L+2b)L^3 / (k v^2)$
H	channel height, m
K	fluid thermal conductivity, $W/m.K$
L	heater width, m
L_1, L_2	Distance from first heater to channel inlet and the last heater to channel exit respectively, m
Nu, \bar{Nu}	Local and average Nusselt number on the heater surface, Eqs. (1), (2)
Pr	fluid Prandtl number, v/α
q	heat flux on the heater surface, W/m^2
Re	Reynolds number, $Re = u_0 L/v$,
Ri	Richardson number, $Ri = Gr/Re^2$
S	distance between each two heaters, m
T	temperature, K
T_0	temperature of the free stream, K
u_0	free stream velocity, m/s
X, Z	distance in horizontal and vertical directions, m
α	fluid thermal diffusivity, m^2/s
β	volumetric coefficient of thermal expansion, $1/K$
θ	dimensionless temperature, $(T-T_0)/(q.L/k)$
ν	fluid kinematic viscosity, m^2/s
ρ	fluid density, kg/m^3

REFERENCES

- 1 Ramadhyani S., Moffatt D., F., and Incropera F., P. "Conjugate Heat Transfer from Small Isothermal Heat Sources Embedded in a Large Substrate," *Int. J. Heat Mass Transfer*, Vol.28, No.10, pp.1945-1952, 1985.
- 2 Incropera, F. P., Kerby, J.S., Moffatt, D.F., and Ramadhyani, S., "Conjugate Heat Transfer from Discrete Heat Sources in a Rectangular Channel," *Int. J. Heat Mass Transfer*, Vol. 29, No. 7, pp. 1051-1058, 1986
- 3 Davalath J., and Bayazitoglu Y., " Forced Convection Cooling Across Rectangular Blocks," *ASME J. of Heat transfer*, Vol.109, pp.321-328, 1987.
- 4 Wadsworth D.C., and Mudawar I., "Cooling of a Multichip Electronic Module by Means of Confined Two-dimensional jets of Dielectric Liquid," *ASME J. of Heat Transfer*, Vol.112, pp. 891-898, 1990

- 5 Kim S. K., and Anand N. K., "Laminar Developing Flow and Heat Transfer Between a Series of Parallel Plates with Surface Mounted Discrete Heat Sources," *Int J Heat Mass Transfer*, Vol.37, No 15, pp.2231-2244, 1994
- 6 Molki, M., Faghri, M., and Ozbay, O., "Correlation for Heat Transfer and Weight Effect in the Entrance Region of an Inline Array of Rectangular Blocks Simulating Electronic Components," *ASME J. of Heat Transfer*, Vol. 117, pp. 40-46, 1995
- 7 Hwang J., and Liou T., "Heat Transfer and Friction in a Low Aspect Ratio Rectangular Channel with Staggered Perforated Ribs on Two Opposite Walls," *ASME J. of Heat Transfer*, Vol. 117, pp. 843-850, 1995.
- 8 Nakayama W., and Park S., H., "Conjugate Heat Transfer from a Single Surface-Mounted Block to Forced Convection Air Flow in a Channel," *ASME J. of Heat Transfer*, Vol.118, pp.301-309, 1996.
- 9 Fowler A. J., Ledezma G. A., and Bejan A., "Optimum Geometric Arrangement of Staggered Plates in Forced Convection," *Int. J. Heat Mass Transfer*, Vol.40, No.18, pp.1795-1805, 1997.
- 10 El-Kady M. S., and Araid F. F., "Natural Convection from a Single Heater in a Vertical Rectangular Enclosure," *Mansoura Eng. Journal (MEJ)*, Vol.23, No 3, pp M25-M40, 1998.
- 11 El-Kady M. S., "Natural Convection from Dual Surface Heat Sources in a Vertical Rectangular Enclosure," *Mansoura Eng. Journal (MEJ)*, Vol 23, No.3, pp.M41-M55, Sept.1998.
- 12 Hlabeck S., and Acharya S., "Laminar Mixed Convection in a Partially Blocked Vertical Channel," *Int. J. Heat Mass Transfer*, Vol.29, pp.1711-1722, 1986.
- 13 Maughan J.R., and Incropera, F. P., "Experiments on Mixed Convection Heat Transfer for Air Flow in a Horizontal and Inclined Channel," *I. J. Heat Mass Transfer*, Vol. 30, pp. 1307-1318, 1987.
- 14 Mahaney, H., Incropera, F., and Ramadhyani, S., "Comparison of Predicted and Measured Mixed Convection Heat Transfer From an Array of Discrete Sources in a Horizontal Rectangular Channel," *Int. J. Heat Mass Transfer*, Vol. 33, No. 6, pp. 1233-1245, 1990
- 15 Kim, S., Sung, H., and Hyun, J., "Mixed Convection From Multiple-Layered Boards With Cross-Streamwise Periodic Boundary Conditions," *Int. J. Heat Mass Transfer*, Vol. 35, No. 11, pp. 2941-2952, 1992
- 16 Papanicolaou E., and Jaluria Y., "Mixed Convection from Simulated Electronic Components at Varying Relative Positions in a Cavity," *ASME J. of Heat Transfer*, Vol.116, pp 960-969, 1994
- 17 El-Kady M. S., and Sultan G. I., "Mixed Convection from a Single Protruding Heat Source in a Horizontal Channel," *Mansoura Eng. Journal (MEJ)*, Vol.23, No 4, December 1988.